Plasma Medicine, 3(1-2): 27–44 (2013)

A Systematic Characterization of a Novel Surface Dielectric Barrier Discharge for Biomedical Experiments

Mareike A. Ch. Hänsch,[1,*] Jörn Winter,[1,2] René Bussiahn,[1] Klaus-Dieter Weltmann[1] & Thomas von Woedtke[1]

[1]Leibniz Institute for Plasma Science and Technology (INP Greifswald), Greifswald, Germany; [2]Center for Innovation Competence plasmatis (italic) at INP Greifswald, Greifswald, Germany

*Address all correspondence to Mareike Hänsch, Leibniz Institute for Plasma Science and Technology, Felix-Hausdorff-Str. 2, 17489, Greifswald, Germany; mareike.haensch@inp-greifswald.de

ABSTRACT: A new surface dielectric barrier discharge (sDBD) based on ceramic materials for improved discharge stability and long-term application was used to investigate the generation of biologically active species in liquids and their effect on planktonic microorganisms. The source was characterized by measurements of dissipated energy, temperature, spectral emission of the discharge, and Fourier transform infrared spectroscopy of the derived working gas. Liquid analysis of plasma-treated samples included the quantitative determination of nitrite, nitrate, and hydrogen peroxide, as well as pH measurements. The biological performance of the discharge was estimated by recording inactivation kinetics for *Escherichia coli*. The obtained results were compared with those of a well-established epoxy sDBD system, which has the same geometrical electrode arrangement but consists of different dielectric materials. Both systems show different physical and chemical performance but very similar antimicrobial effects. This article considers the role of active components of plasma and plasma-induced liquid chemistry in biological effects, and also discusses the main differences between both discharges in detail.

KEY WORDS: atmospheric pressure plasma, surface dielectric barrier discharge, sDBD, plasma-induced liquid chemistry, acidification, nitrate, nitrite, hydrogen peroxide, biological active reactive species, biological efficiency

I. INTRODUCTION

Nowadays, it is widely known that nonthermal atmospheric pressure plasma (APP) is becoming increasingly important in life sciences. Main applications of APP in these research fields include the modification of biorelevant surfaces, decontamination of heat-sensitive materials and tissues, and direct therapeutic use.[1,2] Previous research shows that the biological effects of plasma on cells and microorganisms are mainly mediated via the liquid phase.[3–7] Moreover, plasma treatment of water or physiological saline solutions results in "activated" antimicrobial effective liquids.[3,6,7] Plasma can thus be used in applications other than liquid decontamination. Its effect on liquids raise the possibility of plasma application in the pharmaceutical field to generate, modify, and stabilize pharmaceutical preparations or to support their application.[8,9]

By using a surface dielectric barrier discharge (sDBD) arrangement, Oehmigen *et al.*[3,10,11] showed that plasma generates a variety of reactive species in liquid medium. More-

1947-5764/13/$35.00

over, an antimicrobial effect was shown with this particular plasma source. The sDBD consisted of an epoxy-glass fiber bulk material in which a copper high-voltage electrode arrangement was implemented. The epoxy resin served as a dielectric material.[3,10,11] In this work, we refer to this sDBD arrangement as an epoxy sDBD (Table 1). However, the high-voltage electrode array was covered by an acrylic spray varnish (Plastik 70; CRC Kontakt Chemie and Conrad) to protect the copper electrode against plasma-induced corrosion processes. Unfortunately, this dielectric cover sheath material must be renewed after 45 min of operation. In addition to this inconvenience in use, the continuous loss of the acrylic layer on the electrodes during plasma operation bears the risk of unknown chemical byproducts, which makes stable and reproducible process control difficult.

A new sDBD with the same geometrical arrangement but different dielectric material was subsequently developed to allow long-term application and to minimize corro-

TABLE 1: Comparative summary of characteristics and test results of the ceramic sDBD and the epoxy sDBD

Parameter	Epoxy sDBD[a]	Ceramic sDBD
Dielectric material Electrode material	Printed circuit board: FF4 Copper	Aluminium oxide (Al_2O_3) Silver/platinum conductor paste (Heraeus: C 1076 SD [LPA 609-022])
Dielectric cover sheath	Plastik 70 (CRC Industries GmbH, Germany); plastic coating based on acryl	REACH compliant multilayer dielectric (Heraeus: IP 9117E)
Process gas	Air	Air
Electric parameter • $Voltage_{(peak\text{-}peak)}$ (kV) • Frequency (kHz) • Pulse pattern • Power per single on phase (W) • Power per period (W) • Energy input within 16 s (J)	 10–13 20 See Fig. 2A 12 (Fig. 2A) 1.2 (10 ms); 0.3 (1.6 s) 4.8	 15–18 6 See Fig. 2B 14 (Fig. 2A) 1.4 (1 s) 22.4
Temperature (°C) • Liquid • Gas	 ≤37 30	 ≤37 49
Fluid analysis (mg/L) • Nitrate after 30' PT • H_2O_2 after 30' PT • Nitrite after 10' PT • pH change after 30' PT	 113 18 1.5 2.78	 211 0.72 6.45 2.66
Microbiology 6-log reduction of *E. coli*	 5- to 7-min PT	 5-min PT

Data are compiled from the literature.[3,10,11] PT, plasma treatment.
[a]Data for epoxy DBD compiled from the literature. These data are not compared with Oehmigen. These data are obtained from the corresponding literature.

sion effects. The epoxy-resin dielectric material was replaced with a ceramic material. The embedded high-voltage electrode, made from a silver/platinum conductor paste, was covered with a permanent glass ceramic layer. The electrical operation parameters were adjusted to realize stable and homogenous distributed plasma over the whole electrode surface with the modified materials.

This study aimed to clarify whether these two different DBD plasma sources with identical geometry lead to similar species concentrations in the gas and liquid phases.

Optical emission spectroscopy (OES) and Fourier transform infrared (FTIR) spectroscopy were used to evaluate physical plasma source performance. Quantitative liquid analysis included nitrate, nitrite, and hydrogen peroxide detection, as well as pH measurements. Furthermore, the antimicrobial effect was compared by recording the inactivation kinetics of test microorganisms in liquids.

II. MATERIALS AND METHODS

A. Ceramic sDBD

Our experiments were conducted using a novel sDBD (ceramic sDBD), the schematic of which is shown in Fig. 1. The electrode system is mounted in a gas tight chamber, which fits to the lower shell of a petri dish with a diameter of 55 mm. Gas is supplied from the upper side of the gas chamber and is applied and regulated by using a mass flow controller (MKS Mass-flow, type 647; MKS Instruments Inc.). We used compressed air as the feeding gas, with a flow rate of 0.5 standard liters per minute (slm). However, experiments with other gases or gas mixtures can be realized using this chamber but require adapted electrical operation parameters. The distance between the high-voltage electrode and the 5-mL liquid sample in the petri dish was fixed at 5 mm.

The geometrical electrode layout is identical to the epoxy sDBD arrangement introduced by Oehmigen *et al.*,[3,10,11] but different materials were used to construct the electrode system. A nonstructured, 35-µm-thick sheath of silver/platinum conductor paste on top of a dielectric ceramic disc (Al_2O_3, d = 1.5 mm, Ø 55 mm) acts as a grounded electrode. The high-voltage electrode is arranged on the bottom of the ceramic disc and consists of four concentric rings of silver/platinum conductor paste. The electrically cross-bridged rings have a 0.75-mm width and are separated by a 3-mm gap. A protective coating of dielectric glass ceramic material covers the high-voltage electrode.

Due to altered materials, the electric discharge parameters had to be adjusted to realize stable and reproducible results. The ceramic sDBD was driven by a sinusoidal voltage of 6 kHz frequency. The signal of a function generator (33120A; Agilent Technologies) was amplified and transformed to high voltage, which resulted in a maximum signal amplitude of approximately 17 $kV_{(peak\ to\ peak)}$. To keep the process at low temperature, the plasma was pulsed with 100 ms plasma-on and 900 ms plasma-off times. Hence, an average energy of 1.4 J was dissipated into the plasma per duty cycle, and the power during the plasma-on phase amounted to 14 W. Table 1 summarizes the materials and discharge conditions.

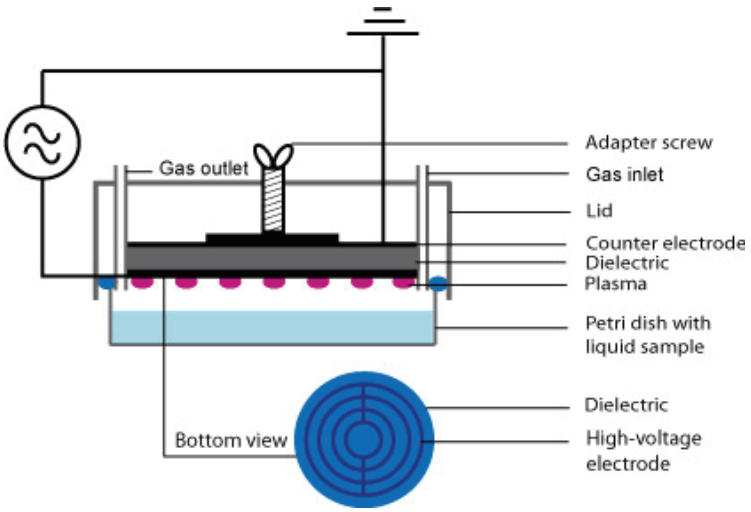

FIG. 1: Schematic of the sDBD arrangement and experimental setup that enables the ignition of atmospheric pressure plasma in air above a liquid sample.

The pulse patterns of both plasma sources are compared with the properties of the plasma source utilized in previous studies[3,10–12] and are illustrated schematically in Fig. 2.

B. Optical Diagnostic of the Plasma

OES was used to characterize the radiation of the discharge. The spectral emission of the ceramic sDBD in the ultraviolet (UV) and visible-near infrared (VIS-NIR) range was analyzed using an AvaSpec-3648-USB2 spectrometer (200–1000 nm, 300 g/mm, 10-µm slit; Avantes Ltd.). Furthermore, the gas temperature in the plasma volume was obtained by a fiber optical sensor (FOT lab kit plus STF-2 probe; Luxtron).

C. FTIR Spectroscopy of the Afterglow

To determine the plasma-produced species, the exhaust gas of the ceramic and epoxy sDBDs was fed into an FTIR spectrometer (Vertex 70v; Bruker). The spectrometer was equipped with a white type multipass cell (A134G/QV; Bruker). The total absorption length and the internal pressure of the cell were set to 3200 cm and 50 mbar, respectively. The ceramic sDBD was investigated for compressed air gas flow rates of 0.5 slm and 1.0 slm over a dry petri dish. For the gas flow rate setting of 0.5 slm, the ceramic sDBD was also operated over a petri dish filled with 5 mL distilled water. To directly compare the ceramic and epoxy sDBDs, FTIR measurement was performed with the identical diagnostic setup on the epoxy sDBD and a compressed air gas flow rate of 1 slm.

The same experimental method was applied for all measurements. After flushing the sDBD with pressurized air at the respective gas flow rate of 0.5 slm or 1.0 slm

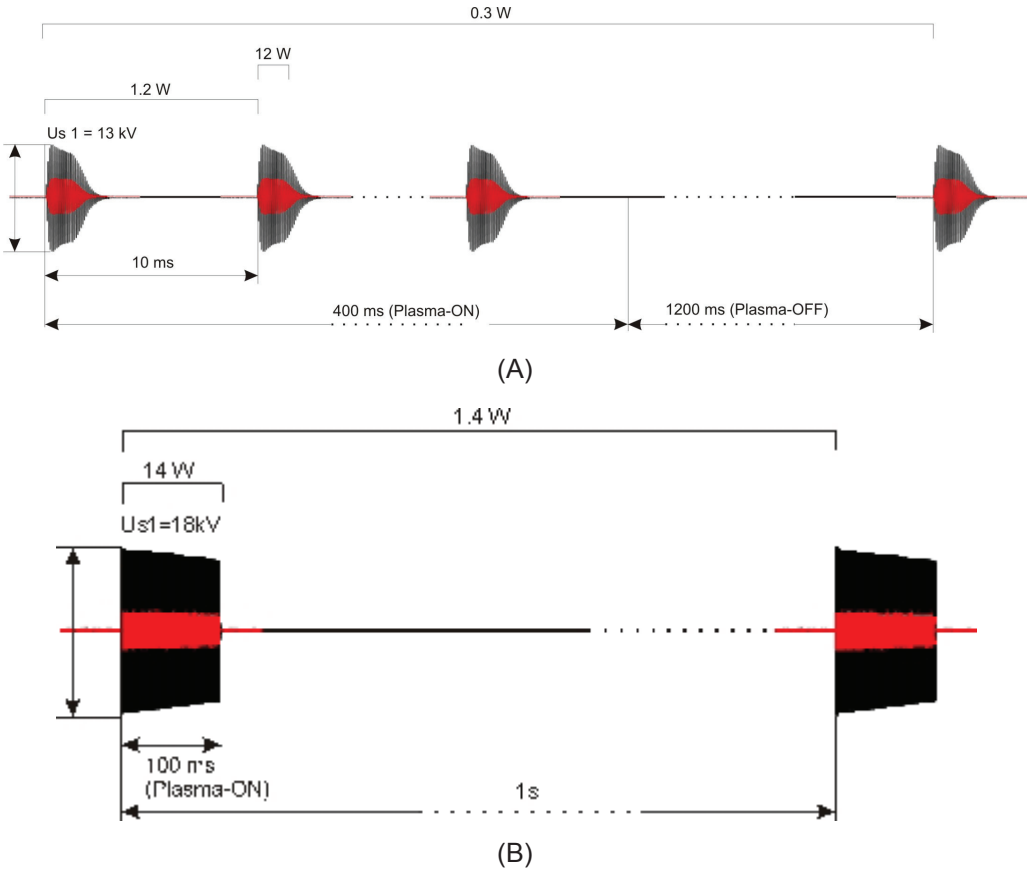

FIG. 2: (A) Electrical pulse pattern of the epoxy sDBD.[3,10–12] (B) Electrical pulse pattern used for the ceramic sDBD.

for 120 min, the background signal (plasma off) was obtained in the spectral interval from 700 cm^{-1} to 2500 cm^{-1}. The spectral resolution was set to 1 cm^{-1}. The plasma was ignited immediately after measuring the background signal. To consider the concentration increase within the multipass cell after plasma ignition, a new FTIR spectrum was obtained every 120 s for the subsequent 10 min. After this time, the absorption peaks in the spectrum did not change, and the concentrations remained constant.

Identification of the species was performed by using the Hitran database and the QMACSoft HT simulation and fit program (neoplas control GmbH). The concentrations of the identified species were obtained from a fitting procedure in which the simulated transmission spectrum was fitted to the measurement using the Levenberg-Marquardt algorithm.

D. Liquid Analytics

Both plasma devices were compared based on the wet-chemical analytical methods and published data described by Oehmigen *et al.*[3,10,11] For this purpose, the identical analytical methods and the same liquid medium were used in this study to characterize the effects of the ceramic sDBD on the liquid phase. This choice excluded possible deviations in analytical results that are caused by a different liquid medium and allowed the direct comparison of both data sets. Furthermore, some of the chemical reactions used by Oehmigen *et al.*[3,10,11] are known to interfere with a high concentration of sodium chloride. Therefore, the 0.85% NaCl solution used for biological assays was disqualified for the chemical analysis. An appropriate sample preparation is required for an accurate quantitative analysis of plasma-treated sodium chloride solutions, and future studies must imply such methods to obtain more specific results. However, the chosen study design allowed the renunciation of such sample preparations. Due to the aforementioned reasons, distilled water served as the sample (5 mL) for all analytical investigations of the liquid phase. Samples were filled in petri dishes and exposed to plasma. Directly after plasma treatment, the pH was measured using a WTW pH meter with a semi-micro pH electrode (Ø 4.5 mm, SENTEK-P13; Sentek Ltd.).

All samples were investigated quantitatively for hydrogen peroxide, nitrate, and nitrite. The molecules were detected by wet-chemical reactions, forming colored products that in turn were photometrically analyzed. A UV/VIS spectrophotometer (SPECORD S 600; Analytic Jena GmbH) was used to record absorption spectra.

Hydrogen peroxide detection was based on the reaction with titanyl sulfate in sulfuric acid solution. The obtained yellow-colored complex (peroxotitanyl sulfate) was measured photometrically at a wavelength of 405 nm.[3,11]

The commercially available Spectroquant test kit (Merck KGaA) was used to determine nitrate ions in liquid samples. This method is analogous to DIN EN 26 777 D10. Nitrite ions react in acidic solution with sulfanilic acid to form a diazonium salt, which in turn reacts with *N*-(1-naphthyl)ethylenediamine dihydrochloride to form a red-violet azo dye. Absorption was measured at 340 nm for quantification of nitrite ions.[3,11]

Nitrate ions were also investigated by using a Spectroquant test kit (Merck KGaA). This method is analogous to DIN 38405 D9. In a 1:1 mixture of phosphoric and sulfuric acid solution, nitrate ions react with 2,6-dimethylphenol to form 4-nitro-2,6-dimethylphenol, which was determined at 525 nm.[3,11]

E. Microbiological Investigations

We evaluated the biological performance of the ceramic sDBD arrangement by using *Escherichia coli* (K12) NCTC 10538 suspended in physiological saline solution according to previously published methods.[3,11] This strain is frequently used as a standard reference to characterize the basic biological effects of plasma treatments. In contrast to analytical experiments biological assays were performed by using physiological sodium chloride solution as suspending agent to avoid lethal osmotic effects.

In this study, the surface spread plate count method using aliquots of serial dilutions of microorganism suspensions according to the European Pharmacopoeia was performed to determine the germicidal effects of the ceramic sDBD.

An overnight culture of *E. coli* in casein/soy flour/peptone broth was centrifuged at 4500*g* for 5 min at room temperature. The pellet was washed and resuspended in sterile physiological sodium chloride solution (0.85% NaCl), resulting in a concentration of 10^6 to 10^7 colony forming units per milliliter (cfu·mL^{-1}). For each sample, 5 mL of the bacteria suspension was added to a petri dish (55 mm diameter) and used for plasma treatment. After plasma treatment, the samples were stored for 15 min at room temperature. Every sample was serially diluted 1:10 with physiological saline containing 0.1% tryptone. One hundred-microliter aliquots from each dilution level were spread in duplicate on casein/soy flour/peptone agar plates. The inoculated agar plates were incubated for 18–24 hours at 37°C. Thereafter, the colony forming units of the test microorganism were manually counted. The detection limit of this experiment was fixed on 10 cfu·mL^{-1}. For every treatment time, the experiment was repeated at least three times. Semi-logarithmic plots depict the inactivation kinetics of *E. coli*.

III. RESULTS

The experimental setup of sDBD generating plasma above a liquid sample is most suitable for systematic investigation of the different phases and components involved in the complex reaction chain of biological plasma effects. The plasma generated on the electrode surface interacts via the gas space between the electrode and liquid surface with the liquid and with cells or microorganisms in the liquid. Fig. 3 shows a typical optical emission spectrum of the discharge in the UV/VIS and NIR spectral range, and reveals the typical bands of the second positive and first negative systems of N_2.

Temperature measurements show that plasma ignition via epoxy sDBD results in a lower gas temperature compared to the ceramic sDBD. However, both discharges lead to a liquid temperature <37° C, which is very convenient for the biological assay.

To determine the differences between both plasma sources, FTIR measurements of the exhaust gas of the ceramic and epoxy sDBDs were performed. Fig. 4 depicts the transmission spectra obtained with the ceramic and epoxy sDBDs for a compressed air gas flow rate of 1.0 slm, as well as the simulated spectra.

Ozone (O_3), nitrogen dioxide (NO_2), nitrous oxide (N_2O), nitric acid (HNO_3), and dinitrogen pentoxide (N_2O_5) are produced in both discharge sources. However, the FTIR spectra reveal that the ceramic sDBD generates generally higher concentrations of these species. Table 2 provides the detailed concentrations. Remarkably, carbon-associated species such as carbon dioxide (CO_2), carbon monoxide (CO), and formic acid (HCOOH) are only found in the epoxy sDBD.

As previously described by several research groups, plasma treatment leads to the formation and time-dependent enrichment of nitrate, nitrite, and hydrogen peroxide as well as to a pH decrease within the liquid phase.[3,11,13,14] In this study, distilled water served as the liquid sample for all analytical experiments except for biological assays. Biological

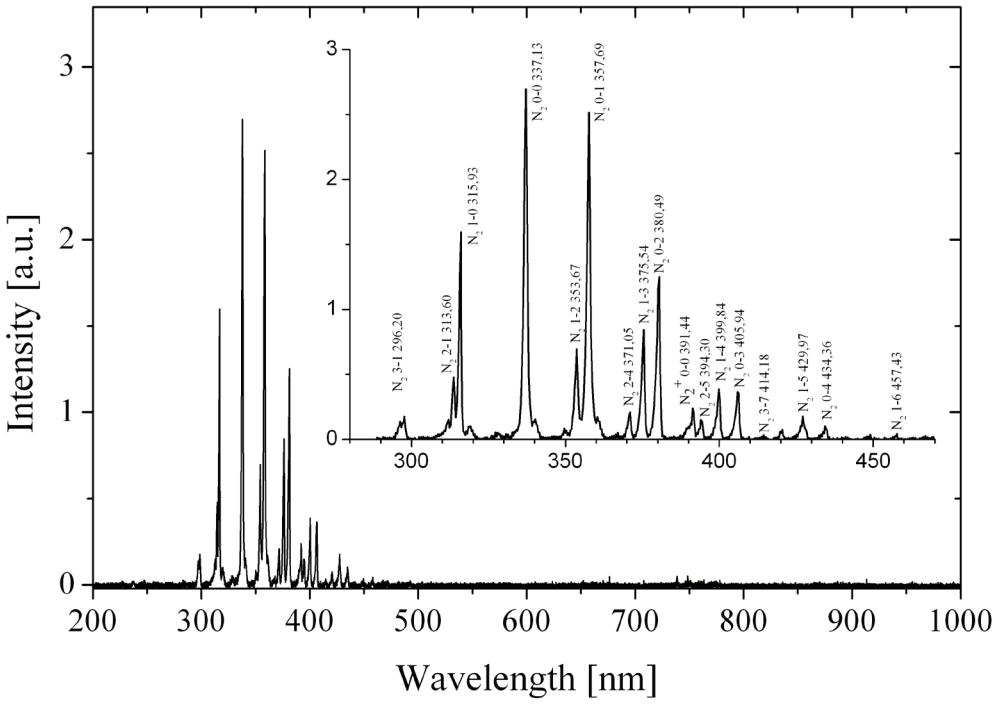

FIG. 3: Optical emission spectrum of the ceramic sDBD discharge in air in UV/VIS and near IR spectral range.

assays were performed by using physiological sodium chloride solution to avoid osmotic effects that can be lethal to bacteria. As previously mentioned, the interfering properties of sodium chloride solution on chemical reactions used disqualified this liquid for wet-chemical analysis. Fig. 5 summarizes our results compared with data compiled from Oehmigen *et al*.[3,10,11] The exposure of plasma to distilled water resulted in a rapid pH decrease from 6.4 to 4.0 within the first minute. With the increased duration of plasma exposure, the pH decreases to 2.6 after 30 min. A time-dependent enrichment of nitrate ions in the liquid was observed. After 15-min plasma treatment, the nitrate concentration reached 207 $mg \cdot L^{-1}$. When the treatment time was doubled to 30 min, no significant further increase in nitrate concentration was obtained (end concentration at 211 $mg \cdot L^{-1}$). The concentration of nitrite increased just within the first 10-min plasma treatment up to approximately 6 $mg \cdot L^{-1}$. Afterward, the amount of nitrite ions remained more or less stable even if the plasma treatment time was increased. In contrast with the observed time-dependent enrichment of nitrate and nitrite, the amount of hydrogen peroxide molecules remained stable at a very low level of <1 $mg \cdot L^{-1}$ over the whole treatment time.

Subsequent biological investigations confirmed the antimicrobial effects of the ceramic sDBD on planktonic microorganisms. Fig. 6 depicts the obtained inactivation kinetics of *E. coli* suspended in NaCl solution. The data represent the mean values of

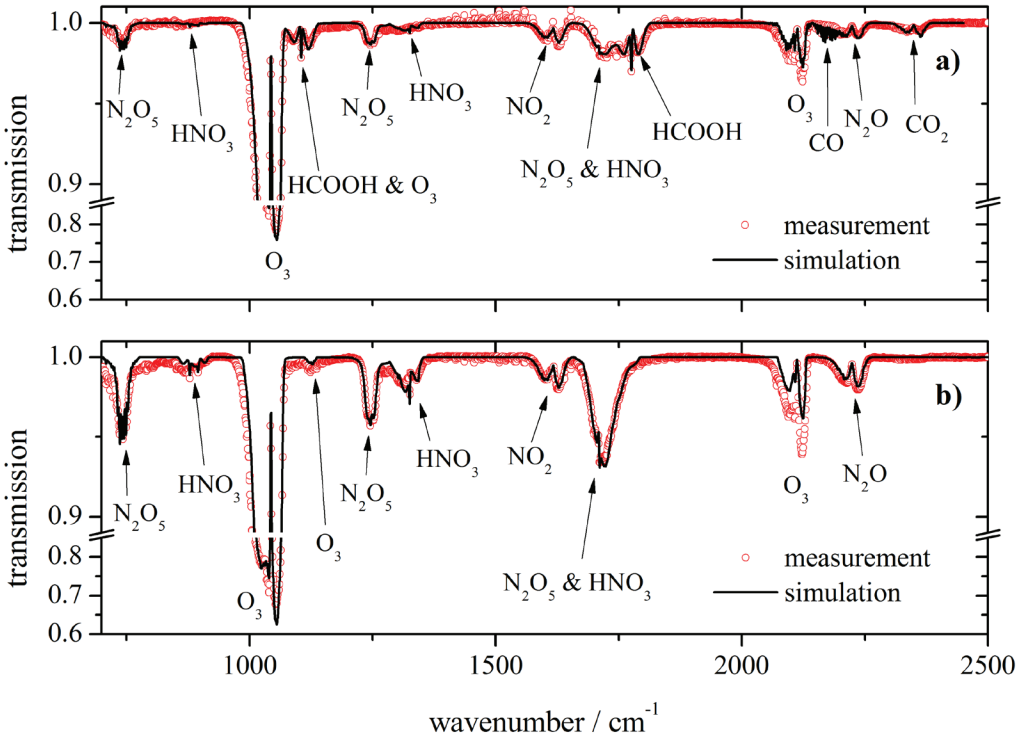

FIG. 4: FTIR spectra of the exhaust gas of the epoxy sDBD (A) and the ceramic sDBD (B) operated with a compressed air gas flow rate of 1 slm.

TABLE 2: Species concentrations detected by FTIR spectroscopy for three different settings for the ceramic sDBD and one setting for the epoxy sDBD

Species	Ceramic sDBD (ppm)			Epoxy sDBD (ppm)
	0.5 slm Air	0.5 slm Air >5 mL H_2O	1.0 slm Air	1 slm Air
Ozone (O_3)	442	159	304	177
Nitrogen dioxide (NO_2)	2.7	6.2	3.5	2.2
Nitrous oxide(N_2O)	7.4	4.0	3.4	1.7
Nitric acid (HNO_3)	14.5	2.2	6.4	1.3
Dinitrogen pentoxide (N_2O_5)	12.2	2.8	6.6	2.1
Formic acid (HCOOH)	—	—	—	4.7
Carbon monoxide (CO)	—	—	—	11.7
Carbon dioxide (CO_2)	—	—	—	0.8
Water (H_2O)	—	164	—	—

Dashes mean corresponding compounds were not detected

at least three independent experiments. For comparison, Fig. 6 also provides the *E. coli* inactivation kinetics resulting from epoxy sDBD treatment as described by Oehmigen

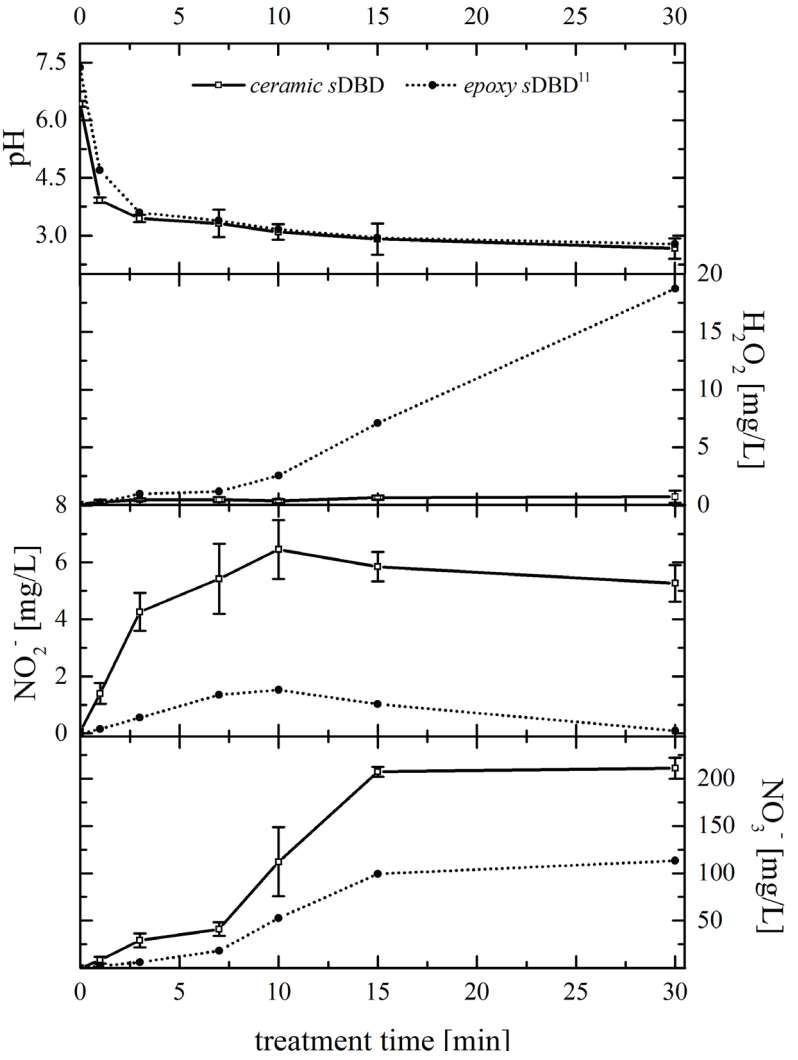

FIG. 5: Concentrations of nitrate, nitrite, and hydrogen peroxide as well as pH values in 5 mL water resulting from 1 to 30 min of epoxy sDBD[11] and ceramic sDBD treatment in air. The presented data are means with standard deviations.

et al.[11] In both cases, a significant inactivation of *E. coli* suspended in NaCl solution was achieved within 3–5 min of plasma exposure. A 6-log reduction in bacteria was observed (i.e., the number of cfu·mL^{-1} fell below the detection limit) with the novel ceramic sDBD after 5-min plasma treatment. The same result was found with the epoxy sDBD after 7 min.[11]

Table 1 provides a comparative summary of all test results with the novel ceramic sDBD and the known epoxy sDBD.[3,10,11]

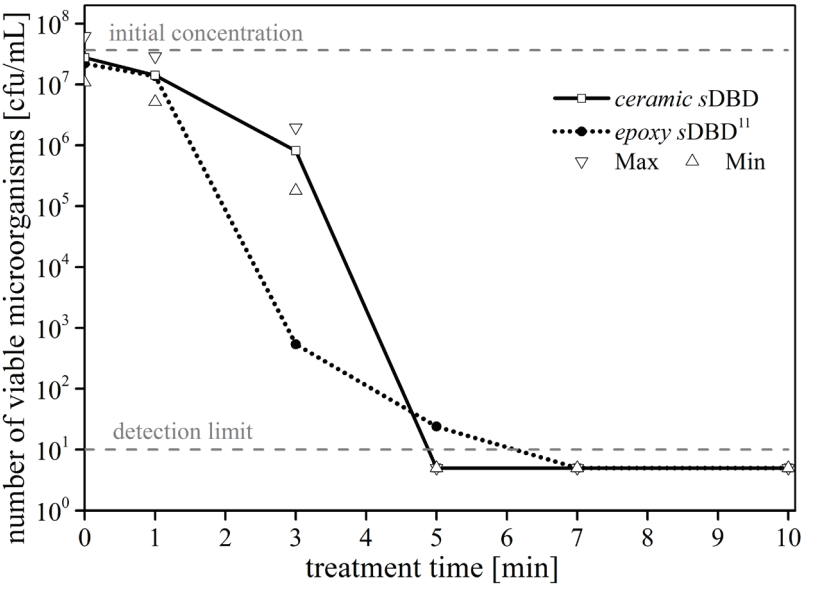

FIG. 6: Inactivation kinetics of *E. coli* suspended in physiological sodium chloride solution dependent on *s*DBD plasma treatment time. Presented data are means (□) with max (▽) and min (△) values resulting from at least three independent experiments. The detection limit is 10 cfu·mL^{-1}. For comparison, the *E. coli* inactivation kinetics resulting from epoxy sDBD treatment as described by Oehmigen *et al*.[11] are also provided.

IV. DISCUSSION

Based on the current scientific evidence, the comparison of different plasma sources on a physical level only is not possible. Therefore, chemical and biological parameters were chosen to compare two different atmospheric pressure plasma sources. For this reason, essential sets of parameters for biological performance were analyzed and described in this study.

Different materials are used to build the new ceramic sDBD device, compared with the epoxy sDBD. Hence, different electrical operation parameters are also necessary to drive the novel ceramic sDBD (Table 1). Despite the slightly higher voltage at lower frequency used for plasma generation in the ceramic sDBD, the power per single plasma-on phase is quite similar in both electrode arrangements. Because of the different pulse patterns, the dissipated average energy is almost five times higher in the novel ceramic sDBD.

To determine whether the different materials and electrical operation parameters affect liquid composition and/or biological reactions, the discharge was investigated with the same diagnostic methods according to Oehmigen *et al.*[3] Therefore, it is important to investigate the effects of the reaction cascade from plasma via gaseous and liquid phases on the microorganism cells.

The systematic analysis of the discharges was started at the plasma phase and OES reveals only the presence of nitrogen emission bands (second positive and first negative system). No emission of hydroxyl molecules (A-X transition) at around 308 nm was detected despite a humid environment and the 4.6-fold higher energy input for the novel ceramic sDBD setup. These findings are in agreement with results by other authors who investigated DBD-generated plasmas in humid air.[3,15] To note, OH(A-X) emission is usually observed if He or Ar are constituents of the gas phase. In the case of DBD air plasma, not enough OH radicals are generated in the excited A state. The absence of OH(A-X) emission does not necessarily mean that no OH radicals are present. The production processes of excited species and the plasma kinetics strongly influence the emission spectrum.[16] The frequency of the possible excitation processes of OH(A) excited molecules (e.g., recombination, direct excitation, and indirect processes including metastable states) as well as quenching (which are both dependent on the gas composition, temperature, humidity, etc.) must be considered for a profound discussion, which was outside the scope of this study.

Analysis of the FTIR spectrum of the exhaust gas generated by novel ceramic sDBD in air under dry conditions (Fig. 4B) shows a similar gas composition as for the epoxy sDBD (Fig. 4A). However, significantly lower concentrations of the detected species O_3, NO_2, N_2O, HNO_3, and N_2O_5 were found in the epoxy sDBD (Table 2). This is most likely due to the higher energy input in the novel ceramic sDBD.

Carbon-related compounds such as CO, CO_2, and HCOOH were measured only in the acrylic covered epoxy sDBD. These species might originate from ambient carbon dioxide, which is present in compressed air at a concentration of approximately 390 ppm. However, because the same gas was used for both discharge sources and carbon-based species were detected only in the epoxy sDBD, it is more likely that the presence of those species is linked to the epoxy sDBD itself. Oehmigen *et al*. previously discussed this fact and concluded that the CO_2 concentration in their measurement originates from a disintegration of the epoxy coating layer by the plasma process.[3] The FTIR measurements obtained in the current study support this hypothesis.

Table 2 provides the results for different gas flow rates. When the gas flow rate decreases from 1.0 slm to 0.5 slm, the concentrations of all detected species, except NO_2, significantly increase. This finding is difficult to interpret without a chemical model. However, the different dilution of plasma-generated species by an altered gas flow rate as well as the complex concentration-dependent chemical reactions both play a significant role.

In addition to the dry condition experiments, the exhaust gas of the ceramic sDBD was also FTIR spectroscopically investigated under wet conditions. The corresponding concentrations are given in Table 2. With regard to the FTIR spectrum (not displayed), we noticed that an intense absorption band of water is present in the spectral range between 1330 and 1980 cm^{-1}. Because special care was given to the background signal determination, the obtained water signal must result from the plasma influence and from the plasma-induced temperature increase of the liquid in particular. Hence, the water

concentration in the plasma-on situation is higher than it was for background measurement. The water concentration was determined to be 164 ppm. All species that are present in the dry setting are also present when the plasma is operated over a liquid. However, the concentrations are different. Except for the NO_2 concentration (6.2 ppm), the concentrations of O_3 (159 ppm), N_2O (4.0 ppm), N_2O_5 (2.8 ppm), and HNO_3 (2.2 ppm) are significantly lower in the humid case. This is due to the higher amount of water, which influences the plasma chemistry as well as the solubility of the reactive gas phase species in the liquid.[17,18]

Liquid analysis reveals acidification as well as enrichment of nitrate molecules in the liquid when the duration of plasma exposure is increased (Fig. 5). Regardless of the ambiguous FTIR results of HNO_3, the increase of nitrate in the liquid indicates that HNO_3 molecules are present in the gas phase and dissolve in water.

In general, the concentrations of nitrite and nitrate as well as the pH decrease in 5 mL water were present at the same order of magnitude with both sDBD arrangements (Table 1). The slightly higher nitrite and nitrate concentrations found with the novel ceramic sDBD treatment might be explained by the higher average energy dissipated by this DBD arrangement. In recent publications, the acidification of liquids following air plasma treatment was attributed to nitrogen-containing compounds such as nitric or nitrous acid.[11,12,19]

The decrease in pH is not exclusively caused by nitrogen-containing compounds. Investigations with plasma generation using the epoxy sDBD in an argon atmosphere showed that a slight decrease in pH is observed without any detection of nitrite or nitrate in the liquid.[12] This finding allows the conclusion that pH changes are caused by more than one compound and are highly dependent on the process gas used. The absence of nitrogen and the exclusive presence of argon give occasion for further theoretical approaches for possible reactions within the liquid phase and require further investigation.

The main and most obvious difference between both discharges is that of hydrogen peroxide concentrations generated in water by the two different electrode arrangements. Whereas hydrogen peroxide concentrations as high as 18 $mg \cdot L^{-1}$ were generated within 30 min of plasma treatment of water with the epoxy sDBD,[1] the hydrogen peroxide concentration remains at a very low level of <1 $mg \cdot L^{-1}$ over the complete treatment time with the new ceramic sDBD (Fig. 5).

Hydrogen peroxide generation in plasma-treated water is usually considered as an indicator of reactive oxygen species (ROS), such as hydroxyl radical ($HO^{\bullet}$), perhydroxyl radical ($HOO^{\bullet}$), or superoxide radical ($O_2^{-\bullet}$), in the plasma/gas phase. When these ROS come in contact with water, they react to H_2O_2 unless other reactants (e.g., organic compounds) are present.[20–22]

On the one hand, the fact that only a low concentration of hydrogen peroxide was detected in water, treated by the novel ceramic sDBD, could point to a relatively low ROS production in the plasma/gas phase caused by the different materials and different operation parameters. On the other hand, radiation at 248 nm,[23] 308 nm,[23] 400 nm,[24] and 405 nm[25] causes photodissociation of H_2O_2 in aqueous liquids. The 4.6-fold higher energy of the ceramic sDBD probably intensifies the radiation on the liquid surface

and causes an increased hydrogen peroxide dissociation, which in turn leads to low concentrations of H_2O_2. Regardless of both possible explanations, the phenomenon of low H_2O_2 levels by ceramic sDBD treatment requires further investigation, including more detailed plasma diagnostics as well as wider liquid analysis. Surprisingly, despite the drastic differences in the materials used, electrical parameters, and obtained results in liquid chemistry, microbiological investigations resulted in similar effects in bacterial inactivation with both sDBD arrangements. In both cases, a 6-log reduction in bacteria growth was found within a 5- to 7-min plasma treatment time of bacterial suspensions. Remarkably, strong germicidal effects were induced when the pH level fell below a certain value (<4). Under these conditions, we observed the following: 1) NO_2^- yields in HNO_2 that are spontaneously disproportionate to $NO^\bullet$, $NO_2^\bullet$, and N_2O_3[3,26]; 2) HNO_2 reacts with H_2O_2 to form peroxynitrous acid (ONOOH)[3,27,28]; and 3) $NO_2^\bullet$ reacts with $OH^\bullet$ radicals to form peroxynitrous acid (ONOOH) and its conjugate base peroxynitrite ($O{=}NOO^-$), which finally decays into NO_3^-.[3,29]

Plasma treatment is able to induce DNA damage and cell wall degradation in microorganisms by oxidative stress.[30,31] *In vitro*, $NO^\bullet$ has proven to be a potent germicidal agent against a variety of microorganisms, including Gram-positive and Gram-negative bacteria. As a broad-spectrum antimicrobial agent, $NO^\bullet$ induces both nitrosative and oxidative stress on biomolecules at cell surfaces. Previous research indicates that cell wall damage is a major contributing mechanism of its cytotoxic effect on microorganisms.[32] Peroxynitrite, another intermediate product of these reactions, is also a strong oxidizing agent that reacts with nucleophiles and electron donors.[33,34] The germicidal effect of plasma-generated peroxynitrite was recently studied[3,5,14,35] and is mainly attributed to lipid peroxidation.[31,32] Because the oxidizing species are not yet clearly identified, $NO^\bullet$ and $O{=}NOO^-$ with their oxidizing properties can be considered as the main cause of DNA damage and cell wall degradation by oxidative stress.[34,36–40]

Even if the reaction chains for antimicrobial reactive nitrogen species (RNS) include $OH^\bullet$ radicals and hydrogen peroxide, these molecules are intermediary reactants for other reactive species such as $NO^\bullet$, $O{=}NOO^-$, and NO_2^-. Furthermore, both plasma treatments did not lead to the minimum inhibitory concentration of H_2O_2 (2505 $mg{\cdot}L^{-1}$) to inactivate bacteria effectively.[3] Therefore, H_2O_2 is excluded as a significant contributing antibacterial agent within the plasma-treated bacterial suspension. Thus, low hydrogen peroxide concentrations obtained with the novel ceramic sDBD (end concentration at 0.72 $mg{\cdot}L^{-1}$) are sufficient to realize the above-mentioned side reactions, whereas higher concentrations of H_2O_2 as found with the epoxy sDBD (18 $mg{\cdot}L^{-1}$) are not essential. Consequently, these findings support that under acidic conditions, nitrogen-containing reactive species such as $NO^\bullet$, $O{=}NOO^-$, and NO_2^- play key roles in bacteria-inactivating mechanisms.

Operating the epoxy sDBD in a pure argon atmosphere did not lead to bacteria inactivation. Under these conditions, neither NO_3^- nor NO_2^- could be detected in liquid analysis.[13] This finding is an additional indication that the germicidal effects must be attributed mainly to low pH and RNS generated by plasma treatment.

V. CONCLUSION

A novel sDBD, using ceramic materials for improved discharge stability and long-term application, was used to investigate the generation of biologically active species in liquids and their effect on planktonic microorganisms. The device was characterized in terms of its physical properties, the chemical composition of the treated water sample, and its biological performance. These results were compared to those of a well-established system (epoxy sDBD[3,10–12]) that has the same geometrical electrode arrangement but consists of different dielectric materials. Due to the latter, specifically adjusted electrical operation parameters are required for each system. We obtained different physical and chemical performances of both systems but similar antimicrobial effects. The specific physical and chemical properties must be attributed to changed dielectric materials and different average dissipated energy. Therefore, we conclude that a comparison of different plasma sources on a physical level and liquid composition are not sufficient to estimate the biological performance.

Consequently, a standardized procedural guideline for complete characterization must be elaborated for evaluation and certification of new plasma sources for biomedical experiments and applications. Such monographs must include plasma diagnostics, liquid analysis, and biological experiments.

This study demonstrates the complexity of the biologically relevant reaction cascade when igniting a surface DBD above a bacterial suspension. The results of this study support the central role of nitrogen-containing reactive species for antimicrobial plasma effects in aqueous medium, whereas H_2O_2 plays a secondary role in bacteria inactivation.

ACKNOWLEDGMENTS

Part of this work was realized within the “Campus PlasmaMed” joint research project and the Centre for Innovation Competence *plasmatis* funded by the German Federal Ministry of Education and Research (grants 13N9779, 13N11188, and 03Z2DN12). Furthermore, financial support from the Ministry of Education, Science, and Culture of Mecklenburg-Western Pomerania is gratefully acknowledged (grant AU 11 038). The authors thank Christiane Meyer for her insight and assistance in various aspects of the project.

REFERENCES

1. von Woedtke T, Metelmann HR, Weltmann KD. Clinical plasma medicine: state and perspectives of *in vivo* application of cold atmospheric plasma. Contrib Plasma Phys. 2014;54:104–17.
2. Weltmann KD, Polak M, Masur K, von Woedtke T, Winter J, Reuter S. Plasma processes and plasma sources in medicine. Contrib Plasma Phys. 2012;52:644–54.
3. Oehmigen K, Winter J, Hähnel M, Wilke C, Brandenburg R, Weltmann KD, von Woedtke T. Estimations of possible mechanisms of Escherichia coli inactivation by plasma treated sodium chloride solutions. Plasma Process Polym. 2011;8:904–13.

4. Reuter S, Tresp H, Wende K, Hammer Mu, Winter J, Masur K, Schmidt-Bleker A, Weltmann KD. From RONS to ROS: tailoring plasma jet treatment of skin cells. IEEE Trans Plasma Sci. 2012;40:2986–93.
5. Naitali M, Kamgang-Youbi G, Herry JM, Bellon-Fontaine MN, Brisset JL. Combined effects of long- living chemical species during microbial inactivation using atmospheric plasma-treated water. Appl Environ Microbiol. 2010;76:7662–4.
6. Traylor MJ, Pavlovich MJ, Karim S, Hait P, Sakiyama Y, Clark DS, Graves DB. Long-term antibacterial efficacy of air plasma-activated water. J Phys D Appl Phys. 2011;44:472001.
7. Julak J, Scholtz V, Kotucova S, Janouskova O. The persistent microbicidal effect in water exposed to the corona discharge. Phys Medica. 2012;28:230–9.
8. von Woedtke T, Reuter S, Masur K, Weltmann KD. Plasmas for medicine. Phys Rep. 2013;530:291–320.
9. von Woedtke T, Haertel B, Weltmann KD, Lindequist U. Plasma pharmacy – physical plasma in pharmaceutical applications. Pharmazie. 2013;68;492–8.
10. Oehmigen K, Hoder T, Wilke C, Brandenburg R, Hähnel M, Weltmann KD, von Woedtke T. Volume effects of atmospheric-pressure plasma in liquids. IEEE Trans Plasma Sci. 2011;39:2646–7.
11. Oehmigen K, Hähnel M, Brandenburg R, Wilke C, Weltmann KD, von Woedtke T. The role of acidification for antimicrobial activity of atmospheric pressure plasma in liquids. Plasma Process Polym. 2010;7:250–7.
12. von Woedtke T, Oehmigen K, Brandenburg R, Hoder T, Wilke C, Hähnel M, Weltmann KD. Plasma-liquid interactions: chemistry and antimicrobial effects. In: Machala Z, Hensel K, Akishev Y, editors. Plasma for Bio-decontamination, medicine and food security. NATO science for peace and security series - A: chemistry and biology. Dordrecht (Germany): Springer; 2012. p. 67–78.
13. Machala Z, Chladekova L, Pelach M. Plasma agents in bio-decontamination by dc discharges in atmospheric air. J Phys D Appl Phys. 2010;43:222001.
14. Brisset JL, Hnatiuc E. Peroxynitrite: A re-examination of the chemical properties of non-thermal discharges burning in air over aqueous solutions. Plasma Chem Plasma Process. 2012;32:655–74.
15. Eto H, Ono Y, Ogino A, Nagatsu M. Low-temperature sterilization of wrapped materials flexible sheet-type dielectric barrier discharge. Appl Phys Lett. 2008;93:221502.
16. Bruggeman P, Verreycken T, Gonzalez MA, Walsh JL, Kong MG, Leys C, Schram DC. Optical emission spectroscopy as a diagnostic for plasmas in liquids: opportunities and pitfalls. J Phys D Appl Phys. 2010;43:124005.
17. Sakiyama Y, Graves DB, Chang HW, Shimizu T, Morfill GE. Plasma chemistry model of surface microdischarge in humid air and dynamics of reactive neutral species. J Phys D Appl Phys. 2012;45:425201.
18. Winter J, Wende K, Masur K, Iseni S, Dünnbier M, Hammer MU, Tresp H, Weltmann KD, Reuter S. Feed gas humidity: a vital parameter affecting a cold atmospheric-pressure plasma jet and plasma-treated human skin cells. J Phys D Appl Phys. 2013;46:295401.
19. Ikawa S, Kitano K, Hamaguchi S. Effects of pH on bacterial inactivation in aqueous solutions due to low-temperature atmospheric pressure plasma application. Plasma Process Polym. 2010;7:33–42.
20. Malik MA, Ghaffar A, Malik SA. Water purification by electrical discharges. Plasma Sources Sci Technol. 2001;10:82–91.

21. Liu F, Sun P, Bai N, Tian Y, Zhou H, Wei S, Zhou Y, Zhang J, Zhu W, Becker K, Fang J. Inactivation of bacteria in an aqueous environment by a direct-current, cold-atmospheric-pressure air plasma microjet. Plasma Process Polym. 2010;7:231–6.
22. Dodet B, Odic E, Goldman M, Renard D. Hydrogen peroxide formation by discharge in argon/water vapor mixtures at atmospheric pressure. J Adv Oxid Technol. 2005;8:91–7.
23. Yu XY, Barker JR. Hydrogen peroxide photolysis in acidic aqueous solutions containing chloride ions. II. Quantum yield of $OH^{\cdot}$ (Aq) radicals. J Phys Chem A. 2003;107:1325–32.
24. Nakamura K, Kanno T, Mokudai T, Iwasawa A, Niwano Y, Kohno M. Microbial resistance in relation to catalase activity to oxidative stress induced by photolysis of hydrogen peroxide. Mirobiol Immunol. 2012;56:48–55.
25. Ikai H, Nakamura K, Shirato M, Kanno T, Iwasawa A, Sasaki K, Niwano Y, Kohono M. Photolysis of hydrogen peroxide, an effective disinfection system via hydroxyl radical formation. Antimicrob Agents Chemother. 2010;54:5086–91.
26. Bryan NS, Loscalzo J, editors. Nitrite and Nitrate in Human Health. Nutrition and Health. New York: Springer; 2011. p. 25–7.
27. Lobachev VL, Rudakov ES. The chemistry of peroxynitrite. Reaction mechanisms and kinetics. Russ Chem Rev. 2006;75:375–96.
28. Lukes P, Dolezalova E, Sisrova I, Clupek M. Aqueous-phase chemistry and bactericidal effects from an air discharge plasma in contact with water: evidence for the formation of peroxynitrite through a pseudo-second-order post-discharge reaction of H2O2. Plasma Sources Sci Technol. 2014;23:15.
29. Mack J, Bolton JR. Photochemistry of nitrite and nitrate in aqueous solutions: a review. J Photochem Photobiol A Chem. 1999;128:1–13.
30. Winter T, Winter J, Polak M, Kusch K, Mäder U, Sietmann R, Ehlbeck J, van Hijum S, Weltmann KD, Hecker M, Kusch H. Characterization of the global impact of low temperature gas plasma on vegetative microorganisms. Proteomics. 2011;11:3518–30.
31. Machala Z, Jedlovsky I, Chladekova L, Pongrac B, Giertl D, Janda M, Sikurova L, Polcic P. DC discharges in atmospheric air for bio-decontamination - spectroscopic methods for mechanism identification. Eur Phys J D. 2009;54:195–204.
32. Deupree SM, Schoenfisch MH. Morphological analysis of the antimicrobial action of nitric oxide on Gram-negative pathogens using atomic force microscopy. Acta Biomater. 2009;5:1405–15.
33. Pryor WA, Cueto R, Jin X, Koppenol WH, Ngu-Schwemlein M, Squadrito GL, Uppu PL, Uppu RM. A practical method for preparing peroxynitrite solutions of low ionic-strength and free of hydrogen peroxide. Free Radic Biol Med. 1995;18:75–83.
34. Radi R, Beckman JS, Bush KM, Freeman BA. Peroxynitrite-induced membrane lipid-peroxidation - the cytotoxic potential of superoxide and nitric oxide. Arch Biochem Biophys. 1991;288:481–7.
35. Machala Z, Tarabova B, Hensel K, Spetlikova E, Sikurova L, Lukes P. Formation of ROS and RNS in water electro-sprayed through transient spark discharge in air and their bactericidal effects. Plasma Process Polym. 2013;10:649–59.
36. Rodenas J, Carbonell T, Mitjavila MT. Different roles for nitrogen monoxide and peroxynitrite in lipid peroxidation induced by activated neutrophils. Free Radic Biol Med. 2000;28:374–80.
37. Zuh L, Gunn C, Beckman JS. Bactericidal activity of peroxynitrite. Arch Biochem Biophys. 1992;298:452–7.

38. Goldstein S, Squadrito GL, Pryor WA, Czapski G. Direct and indirect oxidations by peroxynitrite, neither involving the hydroxyl radical. Free Radic Bio Med. 1996;21:965–74.
39. Murphy MP, Packer MA, Scarlett JL, Martin SW. Peroxynitrite: a biologically significant oxidant. Gen Pharmacol. 1998;31:179–86.
40. Schairer DO, Chouake JS, Nosanchuk JD, Friedman AJ. The potential of nitric oxide releasing therapies as antimicrobial agents. Virulence. 2012;3:271–9.